

Using Visual Texture for Information Display

COLIN WARE and WILLIAM KNIGHT

University of New Brunswick

Results from vision research are applied to the synthesis of visual texture for the purposes of information display. The literature surveyed suggests that the human visual system processes spatial information by means of parallel arrays of neurons that can be modeled by Gabor functions. Based on the Gabor model, it is argued that the fundamental dimensions of texture for human perception are orientation, size (1/frequency), and contrast. It is shown that there are a number of trade-offs in the density with which information can be displayed using texture. Two of these are (1) a trade-off between the size of the texture elements and the precision with which the location can be specified, and (2) the precision with which texture orientation can be specified and the precision with which texture size can be specified. Two algorithms for generating texture are included.

Categories and Subject Descriptors: I.3.3 [Computer Graphics]: Picture/Image Generation – *display algorithms*; I.3.6 [Computer Graphics]: Methodology and Techniques

General Terms: Human Factors

Additional Key Words and Phrases: Gabor functions, information display, scientific visualization, texture, visualization

1. INTRODUCTION

A typical graphic information display, such as a computer screen, provides two spatial dimensions and three color dimensions. For example, we might choose to depict population density, altitude, and rainfall (using three color dimensions) on a map of North America (using two spatial dimensions). Actually, bivariate (let alone trivariate) chromatic maps are notoriously difficult to read [Wainer and Francolini 1980]. To display information with high dimensionality, more display channels are needed. Possible channels include time varying images, representing a third spatial dimension with perspective and other depth cues (a good bet for altitude), and texture, the topic of this paper. Though texture must be portrayed through the space and color dimensions, we easily distinguish, say, the texture of a tweed overcoat from the coat's gross shape and general color.

Authors' address: Faculty of Computer Science, University of New Brunswick, Fredericton, New Brunswick E3B 5A3, Canada.

Permission to copy without fee all or part of this material is granted provided that the copies are not made or distributed for direct commercial advantage, ACM copyright notice and the title of the publication and its date appear, and notice is given that copying is by permission of ACM. To copy otherwise, or to republish, requires a fee and/or specific permission.
© 1995 ACM 0730-0301/95/0100-0003 \$03.50

This paper develops a mathematical model for texture that is based on neurological and psychophysical research. The model is built with data display in mind. It describes the properties of graphical texture primitives called textons [Julesz 1975].

2. NEURAL SPATIAL FREQUENCY DETECTORS

In vision research, most mathematical theories of texture fall into two classes: those based on spatial-frequency analysis, and those based on probability and correlations between neighboring pixels or texture elements. This study is spatial-frequency based. For exposition of the other approach, we mention Beck [1983] and Julesz [1975].

The past two decades have seen much exploration of the response of human vision to sinusoidal or similar gratings (such as in Figure 1) varying in one dimension only, commencing with the now classic papers of Campbell and Robson [1968] and Blakemore and Campbell [1969]. The gratings vary in three dimensions: frequency, orientation, and contrast (amplitude). Based on this research, it was proposed that the human vision system has "channels" selectively sensitive to spatial frequency and orientation. An early conjecture that the vision system might be doing a global Fourier analysis has changed to the view that the vision system examines frequency and orientation on a local basis [Daugman 1984].

2.1 Contrast Sensitivity

Figure 2 shows human threshold sensitivity to grating patterns, in terms of the contrast needed for a texture to be perceived as a function of spatial frequency [Campbell and Robson 1968]. The *frequency* of a pattern is the number of pattern cycles per unit angle (usually degrees) subtended by the eye. We are most sensitive to patterns whose period is approximately 2 cycles/degree. (100 times as much contrast will be needed for a 30-cycles/degree pattern to be perceived as for a 3-cycles/degree pattern.) The sensitivity curve restricts us to a range from roughly 1 to 10 cycles/degree. Assuming 30 pixels/cm at a viewing distance of 75 cm, this translates to a useful wavelength range of approximately 4 to 40 pixels.

2.2 Orientation and Size

A number of electrophysiological and psychophysical experiments indicate that the brain contains large arrays of neurons that filter for orientation and size information at each point in the visual field [Hubel and Wiesel 1968]. These neurons are sensitive to elongated and oriented shapes, for example, those of Figure 3. They also vary in both their preferred orientation sensitivity and preferred spatial sensitivity (they are said to have spatial and orientation tuning). These neurons are held to be responsible for most of the psychophysical results discussed here. Since, according to this model, the output from a single neural processor will not allow discrimination between changes in orientation, size, or contrast of the stimulus pattern, there must be a higher level of processing to discriminate such variation. There is some

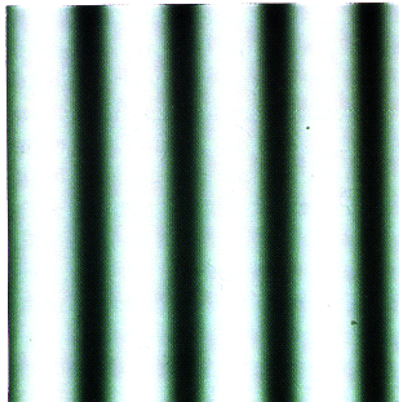


Fig. 1. Sine grating.

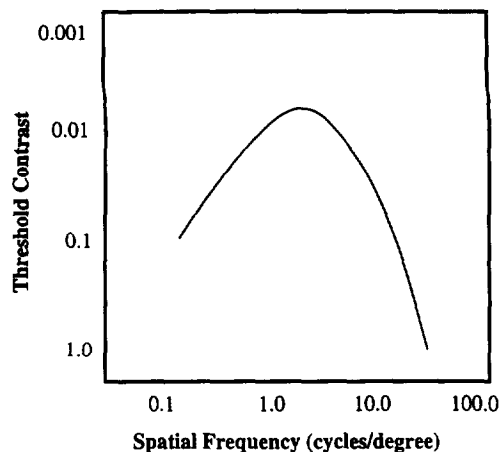


Fig. 2. Spatial modulation threshold sensitivity function of the human visual system. Note the falloff in sensitivity to both high and low spatial frequencies.

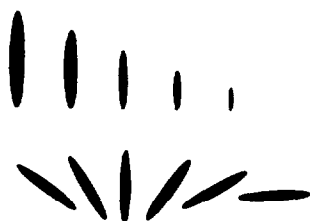


Fig. 3. Neurons are found in the visual cortex that are selectively sensitive to elongated and oriented shapes such as these.

evidence for a higher level of processing that separates adjacent areas filled by different textures [Chua 1990; Sagi 1990].

The basic neural detectors are broadly tuned with respect to orientation and size. Sensitivity in orientation appears to be about $\pm 30^\circ$ [Blake and Holopigian 1985; Daugman 1984]. The width of the spatial frequency band selected by a detector may be a size change by a factor of ten [Wilson and Bergen 1979] or a factor of four [Daugman 1984], and the number of

frequency channels has been variously estimated as between four and ten [Caelli and Moraglia 1985; Harvey and Gervais 1981; Wilson and Bergen 1979]. However, higher discrimination resolutions are achieved by the neural differencing of the outputs of broadly tuned detectors, much as fine color discrimination is achieved neurally by differencing of the outputs of the cone receptors. The resolvable size difference (1/frequency) appears to be about 1/8 of an octave (a size change of 9 percent), which yields 24 resolvable size steps for the useful 3-octave range [Caelli and Bevan 1983; Caelli et al. 1983; Heeley 1991]. The resolvable orientation difference appears to be approximately 5° [Caelli et al. 1983]. Observers have a higher ability to discriminate oriented patterns that are closer to vertical and horizontal than to oblique orientations. This is attributed to fewer, more broadly tuned neural detectors sensitive to oblique orientations [Mitchell et al. 1967].

3. GABOR FUNCTIONS

Most of the theoretical accounts of the textual perception discussed above are based on a class of neurons, originally called “bar” and “edge” detectors, found in the visual cortex of mammals [Hubel and Wiesel 1968]. (David Hubel and Torstein Wiesel received Nobel prizes in 1981 for pioneering this work.) Mathematical models of these have been developed [Garner and Felfoldy 1970; Heeley 1991]. A mathematical model based on the Gabor function accounts for a variety of experimental results [Chua 1990; Jones and Palmer 1987; Marcelja 1980; Nothdurft 1991; Porat and Zeevi 1989].

A Gabor function is the product of a Gaussian envelope and a sinusoidal grating:

$$\exp(-\frac{1}{2}(x^2 + y^2)) \exp(jf_0 y), \quad (1)$$

where x and y are space coordinates, f_0 is a frequency, and $j = \sqrt{-1}$, as usual. The Gaussian window defines location by limiting extent; the sinusoid defines grating orientation and frequency.

The Gabor function (1) is complex; we use either the real part (cosine Gabor),

$$\exp(-\frac{1}{2}(x^2 + y^2)) \cos(f_0 y), \quad (2)$$

or the imaginary part (sine Gabor),

$$\exp(-\frac{1}{2}(x^2 + y^2)) \sin(f_0 y). \quad (3)$$

Figure 4 parts a and b illustrate the cosine (2) and sine (3) Gabor functions, respectively.

In human neural receptive fields, the window and cosine components tend to be coupled so that low-frequency cosine components have large windows and high-frequency components have small windows. Caelli and Moraglia [1985] did a study to assess the ratio of window width to spatial frequency of the grating component. They concluded that the window profile, to $1/e$ decay values, spans approximately two cycles of the grating: This happens when $w_0 = \pi/\sqrt{2}$.

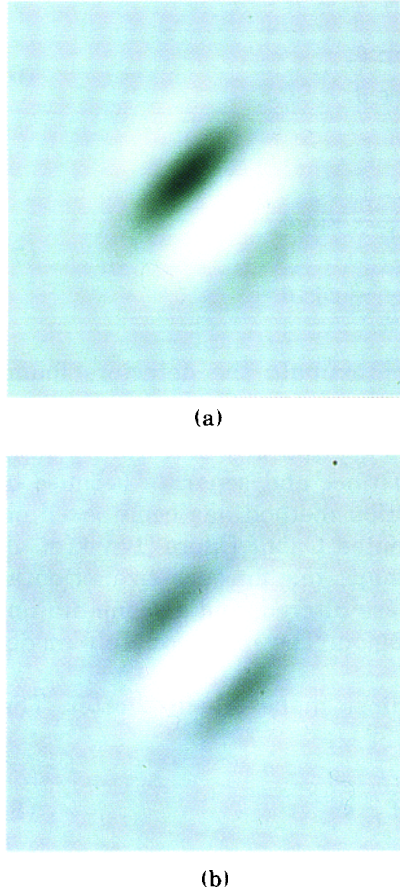


Fig. 4. (a) Cosine and (b) sine Gabors. The cosine Gabor is symmetrical. However, the difference is not obvious at first glance, indicating that we are not very sensitive to phase difference.

The window of (1)–(3) is centered at the origin and is circular in outline. We want to do transformations, move the window, change its size, elongate it to an ellipse, and rotate it to other orientations.

Changing origin is done by replacing x and y by

$$\begin{aligned}x' &= x - x_0, \\y' &= y - y_0.\end{aligned}\quad (4)$$

The size of the window can be adjusted by multiplying x and y by scaling factors. Since bar and edge detectors can be elongated and have an elliptical rather than a circular outline, we may want to apply different scalings to x and y :

$$\begin{aligned}x' &= \frac{x}{a}, \\y' &= \frac{y}{b}.\end{aligned}\quad (5)$$

Rotation is done the usual way:

$$\begin{aligned}x' &= x \cos \theta - y \sin \theta, \\y' &= x \sin \theta + y \cos \theta.\end{aligned}\quad (6)$$

Combining all of these transformations,

$$\begin{aligned}x' &= \frac{x - x_0}{a} \cos \theta - \frac{y - y_0}{b} \sin \theta, \\y' &= \frac{x - x_0}{a} \sin \theta + \frac{y - y_0}{b} \cos \theta.\end{aligned}\quad (7)$$

These transformed Gabor functions can approximate the detectors found electrophysiologically. Figure 4 features pictures of some Gabor functions.

Other evidence for the appropriateness of the Gabor model comes from studies of texture segmentation. When a photograph of a natural scene is examined, different patches appear to be distinct and separate because of their texture. A successful texture segmentation method has been based on parallel processing by a set of sized and oriented Gabor filters [Bovik et al. 1990]. The output of this process is a set of maps, one for each size-orientation combination. These maps are then low pass filtered, and a segmentation is based on the dominant map for a given region. The results closely model human segmentation.

Rewriting formulas in vector form sometimes makes them shorter. The vector form of (1) becomes

$$\exp\left(-\frac{1}{2}\|\vec{\mathbf{x}}\|^2\right) \exp\left(j\vec{\mathbf{f}}_0 \cdot \vec{\mathbf{x}}\right), \quad (8)$$

where $\vec{\mathbf{x}} = (x, y)$, $\vec{\mathbf{f}}_0 = (0, f_0)$ for a grating in the y direction, and $(f_0, 0)$ for a grating in the x direction.

4. GABOR DETECTORS AND STIMULI

Detection is modeled as an inner product between detector and signal, making the response of detector D to signal S

$$\text{response} = \int D(\vec{\mathbf{x}})S(\vec{\mathbf{x}}) d\vec{\mathbf{x}}. \quad (9)$$

A detector will be more sensitive to some signals than to others. It is reasonable to model this sensitivity as

$$\text{sensitivity} = \frac{\text{response}}{\|S\|}. \quad (10)$$

(The norm of a function is taken as the square root of the inner product of the function with itself.)

Sensitivity is highest for a signal of the same shape as the detector. This

follows from the Cauchy-Schwartz inequality,

$$\left| \int D(\vec{x})S(\vec{x}) d\vec{x} \right| \leq \|D(x)\| \|S(x)\|, \quad (11)$$

equality obtaining when D and S are the same shape. For example, a Gabor cosine detector is optimal for the same Gabor cosine stimulus, but works poorly with its dual Gabor sine stimulus. Thus, the optimal texton for a Gabor detector is a Gabor texton, and vice versa.

5. SPACE-FREQUENCY DUALITY

We can represent an image in either the space or frequency domain. Both are relevant in a vision system entailing frequency sampling localized in space [Daugman 1984]. The second dogma of Barlow [1972] asserts that the visual system is simultaneously optimized in both spatial and frequency domains. We should consider space and frequency together, looking simultaneously at the spatial form and its frequency dual (Fourier transform) of any detector or textons. A convenient model should move easily between space and frequency; Gabor functions do just this since the Fourier transform of any Gabor function is another Gabor function. It has been claimed [Daugman 1985] that the Gabor function is optimal in that it jointly optimizes sensitivity in space and frequency domains as Barlow's dogma would require.

5.1 Gabor Functions in Space and Frequency

The frequency image of a Gabor function is another Gabor function with the roles of space and frequency reversed. For location \vec{x}_0 and frequency \vec{f}_0 , the space form is a function of the space vector \vec{x} ,

$$\exp\left(-\frac{1}{2}\|\vec{x} - \vec{x}_0\|^2\right) \exp\left(j\vec{f}_0 \cdot (\vec{x} - \vec{x}_0)\right), \quad (12)$$

and the frequency form is a function of the frequency vector \vec{f} ,

$$\exp\left(-\frac{1}{2}\|\vec{f} + \vec{f}_0\|^2\right) \exp\left(j\vec{x}_0 \cdot (\vec{f} + \vec{f}_0)\right), \quad (13)$$

obtained by exchanging x and w throughout.

Any geometric transformation of a space-domain function induces a dual transformation in its frequency-domain Fourier transform. These dualities are listed in Table I. Formulas corresponding to these are in the Appendix.

The real and imaginary parts of (12) each consist of two Gabors,

$$\begin{aligned} \exp\left(-\frac{1}{2}\|\vec{x}\|^2\right) \cos(\vec{f}_0 \cdot \vec{x}) &= \exp\left(\frac{1}{2}\|\vec{x}\|^2\right) \frac{\exp(j\vec{f}_0 \cdot \vec{x}) + \exp(-j\vec{f}_0 \cdot \vec{x})}{2}, \\ \exp\left(-\frac{1}{2}\|\vec{x}\|^2\right) \sin(\vec{f}_0 \cdot \vec{x}) &= \exp\left(-\frac{1}{2}\|\vec{x}\|^2\right) \frac{\exp(j\vec{f}_0 \cdot \vec{x}) - \exp(-j\vec{f}_0 \cdot \vec{x})}{2}. \end{aligned} \quad (14)$$

Table I. Dual Transformations

Space domain	Frequency domain
Change position	Multiply by frequency grating
Multiply by frequency grating	Change position
Scale uniformly by s	Scale uniformly by $1/s$
Scale axes by different factors	Scale axes by reciprocal factors
Rotate by θ	Rotate by θ
Scale amplitude by c	Scale amplitude by c

These are the sum and difference, respectively, of two complex exponentials, so the Fourier transforms feature two windows:

$$\frac{\exp\left(-\frac{1}{2}\|\vec{\mathbf{f}} + \vec{\mathbf{f}}_0\|^2\right) + \exp\left(-\frac{1}{2}\|\vec{\mathbf{f}} - \vec{\mathbf{f}}_0\|^2\right)}{2}$$

and

$$\frac{\exp\left(-\frac{1}{2}\|\vec{\mathbf{f}} + \vec{\mathbf{f}}_0\|^2\right) - \exp\left(-\frac{1}{2}\|\vec{\mathbf{f}} - \vec{\mathbf{f}}_0\|^2\right)}{2j}. \quad (15)$$

5.2 Trade-Offs in Information Density: An Uncertainty Principle

Daugman [1985] showed a fundamental uncertainty principle relating to perception of position, orientation, and frequency: Given a fixed number of detectors, resolution in size (1/frequency) can be traded for orientation and position. The same principle applies to the synthesis of texture for data display. In order to convey precise information in the frequency domain, the texton must be relatively large, but this makes it take up a lot of room and, hence, reduces information in the space domain. A gain in one is a loss in the other.

Figure 5 illustrates the trade-offs in terms of information display when scale is manipulated. Figure 5a and b shows that enlargement of the Gaussian envelope in the space domain shrinks the envelope in the frequency domain; this means that a low spatial information density can be coupled with a precise specification of texture size, but both are not simultaneously possible. Figure 5c and d shows that stretching the Gaussian envelope perpendicular to the bands of the sine grating increases the wavelength specificity, while decreasing the orientation specificity, and that the converse is true. Thus given a constant data density, either orientation or size can be specified precisely, but not both. Note that the trade-offs between texton size, texton orientation, and information density are general in that they apply to any texture elements and not only to Gabor textons.

6. THE OSC TEXTURE SPACE

So far, we have made some observations concerning the suitability of a simplified class of Gabor functions as primitives in the generation of texture. We only need to add an amplitude or a contrast term c in order to provide an

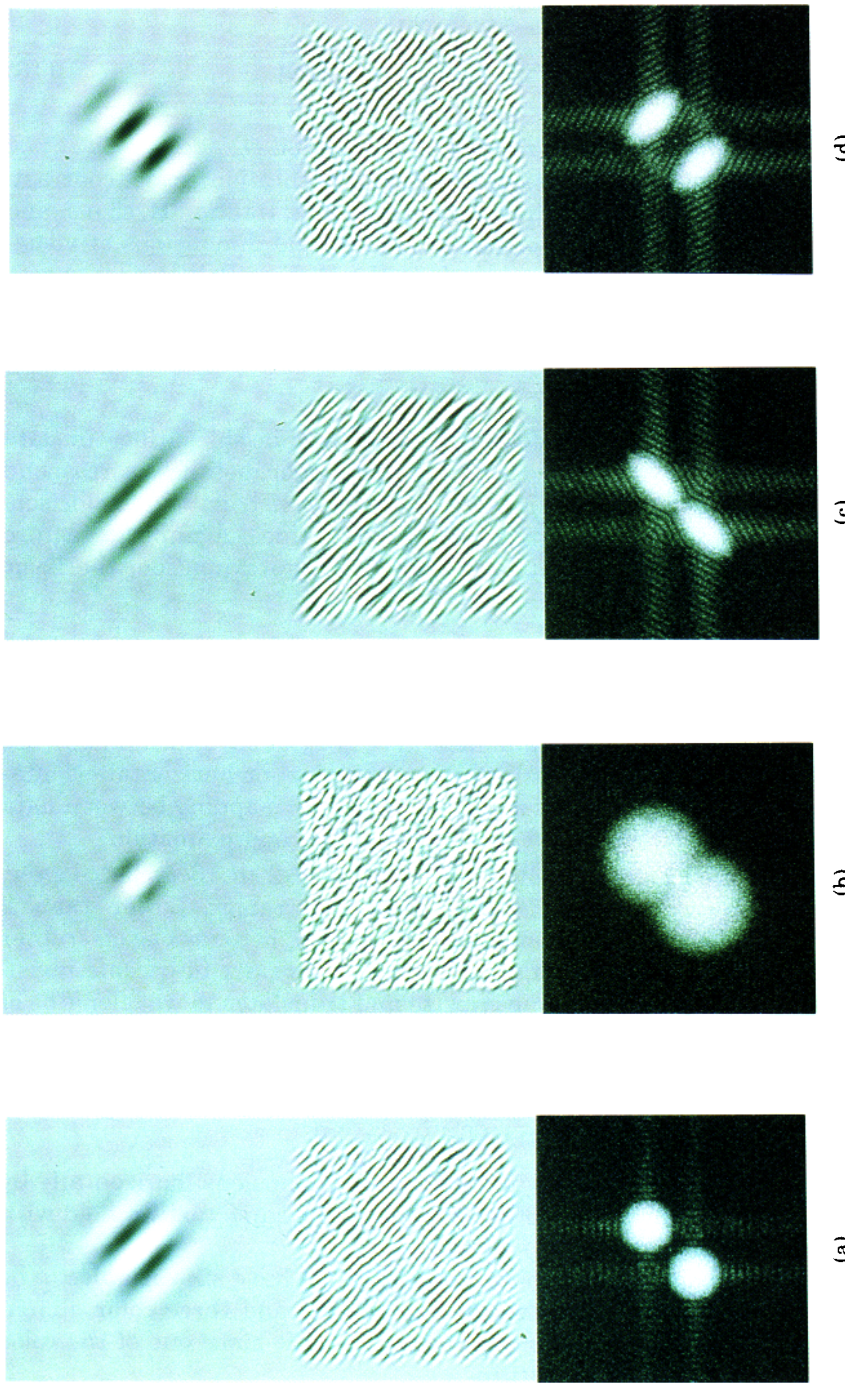


Fig. 5. (a) and (b) show scaling the Gaussian envelope for a constant cosine grating effects the Fourier transform. A larger space-domain sampling results in a smaller frequency domain sampling; in other words, the frequency is specified more precisely. (c) and (d) show how stretching the Gaussian envelope with a constant area affects the Fourier transform. If stretched across the grating orientation is specified more precisely, size is specified less precisely; if stretched along the grating, the converse is true.

ideal texton with three parameters controlling orientation (O), size (S), and contrast (C):

$$c \exp\left(-\frac{1}{2}\|s\mathbf{R}\vec{\mathbf{x}}\|^2\right) \exp\left(\frac{\pi}{\sqrt{2}}s\vec{\mathbf{f}}_0\mathbf{R}\vec{\mathbf{x}}\right). \quad (16)$$

Here, R is a rotation matrix that rotates to orientation O.

We call the space of these functions the OSC (orientation, scale, contrast) texture space, and we claim that the three parameters, rotation R , size s , and contrast c , capture the principal orderable, perceptual dimensions of visual texture in a way that is easy to use, much as the HSV or RGYB color spaces [Smith 1979; Ware and Cowan 1990] make color easily accessible to computer graphics for the purposes of information display.

6.1 Scaling the OSC Dimensions

Uniform color spaces have been found to have considerable utility in data display. They transform color space so that equal metric distances correspond to perceptual distances and, in this way, allow the construction of color sets that more correctly represent a given set of data values. A uniform texture space is also a possibility, and at least to a first approximation, the basic scalings are clear.

- Orientation.* This is scaled linearly over a range of 0 to π . Because of the two-axis symmetry of Gabor textons, only 180° of orientation are available. However, if a directional texton, for example, a fish shape, is used, then 360° will be unambiguously available. There is evidence that humans are less sensitive to oblique orientation than to vertical or horizontal orientation. However, this departure is small, and a linear mapping between data and orientation is probably good enough for a first approximation.
- Size.* This is scaled exponentially over a range of 2 to 16 cycles/degree. There is a limited practical spatial frequency range: Lower than 2 cycles/degree, the textons are so large that they become objects rather than texture elements; higher than 16 the textons start to become invisible. This allows for three doublings in size and translates to wavelengths of between 1/2 and 1/16 degrees of visual angle [Ware and Knight 1992].
- Contrast (amplitude).* Contrast should be scaled exponentially [Wyszecki and Stiles 1982]. A reasonable useful range for $c = (I_{\max} - I_{\min}) / (I_{\max} + I_{\min})$ would appear to be $0.1 \leq c \leq 1.0$.

Figure 6 shows a texture field modulated in two dimensions, horizontally by size and vertically by orientation. Figure 7 shows the same texture field with contrast modulated radially.

If our texture model is correct in its basic form, we have six variables to be used to display map data: three texture dimensions and three color dimensions. Of these six only five are simultaneously usable since one of the color dimensions must be applied to texture.

It should be understood that this is not intended to be a complete model of texture perception. Texture has a large number of degrees of freedom, and

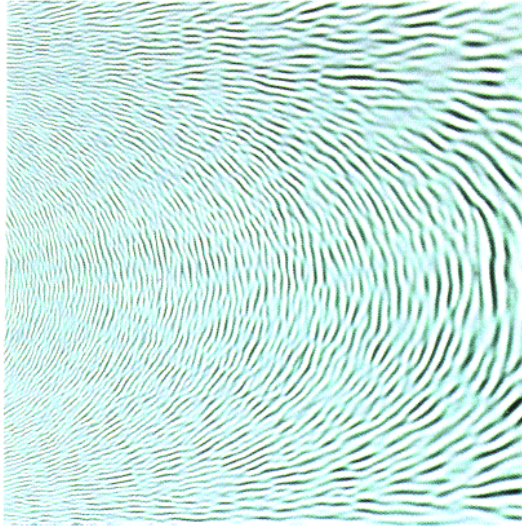


Fig. 6. Texture field swept horizontally by size and vertically by orientation. Algorithm 1 was used to generate this pattern.

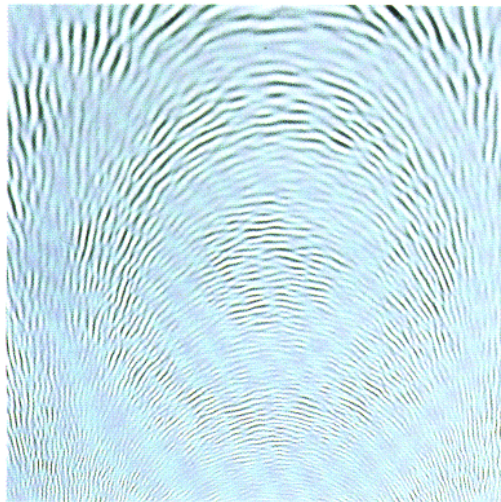


Fig. 7. Texture field swept horizontally by size, vertically by orientation, and radially by contrast. Algorithm 1 was used to generate this pattern.

other factors such as regularity, phase information, local symmetry, and combinations of spatial frequencies are all perceptually significant. The claim here is that these three dimensions of texture are primary in the sense that variation according to these dimensions will be more visible than variation according to other dimensions. We also claim that these dimensions are perceptually ordered: A medium-contrast texture will lie between a high- and a low-contrast texture; a medium-grained texture will lie between a large- and small-grained textures; a texture oriented at 45° will clearly lie between textures oriented at 0° and 90°.

7. TEXTURE SYNTHESIS

One convenient way to make textures is to put points in the space the texture is to occupy and then to place a texton at each point. (Mathematically, this is a convolution between a point process and a basic shape.) The points can be placed in a regular pattern, rectangular, hexagonal, or whatever; or points can be placed at random, by a Poisson or other process. The Poisson process has two advantages over regular grids:

- (1) It is isotropic: Unlike a rectangular pattern, no particular orientation is emphasized.
- (2) A regular grid generates aliasing, that is, beat frequencies between the frequency of the grid and that of the Gabor detector; the Poisson process, lacking clearly defined frequencies, does not.

7.1 Texture Synthesis Algorithms

Assuming that the OSC model is essentially correct, we are left with the problem of synthesizing textures in such a way that the orientation, size, and contrast of a texture field can be varied continuously. An algorithm is required with these design constraints:

- (1) A texton at a particular location should be sized, oriented, and contrasted with its background according to the local information to be displayed (from between one and three univariate maps).
- (2) Texton density should be inversely related to texton size so that the ratio of texton to background is constant.
- (3) Textons should be randomly distributed (to avoid aliasing artifacts).

We present two such algorithms. The first is designed to use Gabor functions as primitives, while the second is designed to use other patterns as textons. In both algorithms we sample the image plane randomly using a modified Poisson process, and splatter textons shaped and scaled according to the local data attributes. Our two methods differ in the way splatter density is made inversely proportional to the texton size and in the kind of textons we use.

7.2 Algorithm 1

Algorithm 1 (Figure 8) is similar to the spot noise method developed by van Wijk [1991], except that far fewer texture stampings are necessary because the Gabor primitive is smooth. The algorithm uses a Poisson sampling of the data plane modified so that the density is inversely proportional to the texton size.

Modifications can be made to this algorithm to increase speed. We have found it advantageous to precompute a two-dimensional array of Gabor textons varying size in one dimension and orientation in the other, using symmetry to reduce table storage. Contrast is applied in a last pass through **Texture buffer**, prior to converting it into an 8-bit image for display. Figure

```

Major Variables
DisplayBuffer          /* A two dimensional array the size of the data array      */
TextureBuffer          /* A two dimensional array the size of the data array      */
p:                      /* A position in the DisplayBuffer                         */
n_samples              /* The number of samples of the data plane                */
MapA, MapB, MapC        /* Two dimensional arrays containing the data to be represented. */
                           /* Any two of these may be null (and replaced by a constant.) */

External procedures
RandomPixel            /* RandomPixel returns a random pixel position           */
UniformRandom           /* UniformRandom returns a random variable of [0,1]       */

begin Texture
  Zero TextureBuffer
  /* Sum Gabor Textons into the TextureBuffer */
  for i ← 1 to n_samples
    p ← RandomPixel(p)
    TextonArea ← texton area specified according to MapA
    /* Make texton density vary inversely with texton size */
    if UniformRandom() < (Area of Smallest Texton)/TextonArea
      Size      textons according to MapA
      Orient    textons according to MapB
      Contrast  texton according to MapC
      Sum Gabor texton into TextureBuffer centered at position p
    end if
    /* Scale the texture for display typically to the integer range (0..255) */
    FrameBuffer ← Mean Luminance + TextureBuffer × Luminance_scale
  end for
end Texture

```

Fig. 8. Algorithm 1.

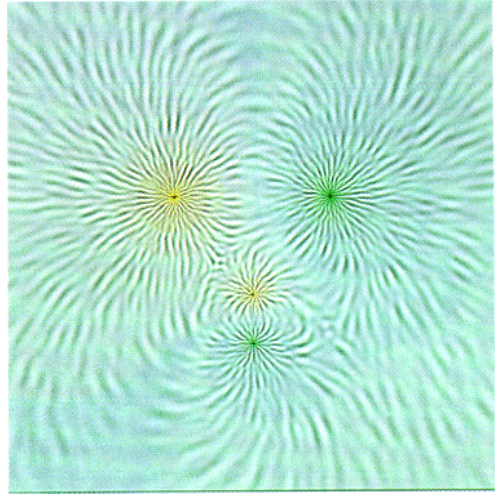
9 illustrates the magnetic field produced by two dipoles using Algorithm 1. In this figure field orientation is mapped to texton orientation, and field strength is mapped to the inverse of texton size and texton contrast.

In our experiments with synthetic texture, we have used formula (16) as the texture primitive. However, if better size resolution were, for example, desired the parameters described in eq. (6) could be added to trade off resolution in one texture parameter for another. Using Gabor primitives results in a “pure” texture according to the theory outlined in this paper, and this texture should be optimal in the sense of providing an unambiguously oriented, sized, and contrasted texture. However, the basic model applies to any texture created with elongated and oriented textons, although the results may be less perceptually distinct. Non-Gabor textons have an advantage in the possibility of using texton shape to highlight qualitative aspects of the data. Thus, an elliptical texton might be used in one region to distinguish it from another region covered with rectangular textons.

7.3 Algorithm 2

The two-pass algorithm in Figure 10 is designed to synthesize textures with simple geometric textons. The first pass is used to establish texton spacing,

Fig. 9. Shows the magnetic field generated by two dipoles. Field orientation is mapped to texture orientation, and field strength is mapped to texture contrast and inversely to texture size. Texture is displayed using the luminance dimension, while field potential is displayed by a color sequence.



and a second pass is used to draw them. On the first pass, pixels in the frame buffer are sampled in a random order, and a **texton** of the appropriate size and orientation is displayed only if that location has not been already covered by a previously drawn texton. A **Hits_buffer** array records the center locations of textons that are drawn. The purpose of the first pass is to establish the density and separation of textons according to the constraints. On the second pass, the textons are drawn according to the locations stored in the **Hits_buffer**, but at a smaller size (usually half).

8. EXAMPLE: AN ILLUSION

We present one concluding example that illustrates both the texture that results when orientations are randomized and some of the theoretical evidence that human neural processes respond to texture size. Texture-size contrast is a phenomena where an isolated region of texture is perceptually distorted by the texture of surrounding regions. This phenomenon is thought to be caused by lateral interactions between frequency selective regions of the visual cortex [Blakemore et al. 1970]. In Figure 11 the background texture is swept from left to right in size. There are two patches of identically sized textons embedded in this background. The granularity of the patch on the large texton background appears finer than the granularity of the patch on the small texton background. The relevance of this demonstration from the point of view of information display is that texture contrast can cause distortions in readings of texture-coded data, just as color contrast can cause distortions in color-coded data [Ware 1988].

9. SUMMARY AND CONCLUSIONS

We have developed a model of the principal orderable dimensions of visual texture. These dimensions are orientation, size, and contrast. The strongest

```

Major Variables
DisplayBuffer      (* A two dimensional array the size of the data array      *)
HitsBuffer        (* A two dimensional array the size of the data      *)
p, r              (* Positions in the display or hit buffers      *)
MapA, MapB, MapC  (* Two dimensional arrays containing the data to be represented.      *)
                    (* Any two of these may be null.      *)

begin Texture
  Zero HitsBuffer and DisplayBuffer
  (* First pass to establish texton spacing *)
  for p over all pixels do
    r ← Random(p)  (* Random is a pseudo-random permutation mapping p      *)
                    (* into pixel indices. This assures "random" order.      *)
    if DisplayBuffer[r] = 0 then
      Size texton according to MapA
      Orient texton according to MapB
      Draw a twice texton sized block of 1's centered at position r into the DisplayBuffer
      HitsBuffer[r] ← 1
    end if
  end for
  (* Second pass to create the image. *)
  Zero DisplayBuffer
  for p over all pixels do
    if HitsBuffer[p] = 1 then
      Size texton according to MapA
      Orient texton according to MapB.
      Contrast texton according to MapC.
      Draw texton with size, orientation, and contrast appropriate to position p
    end if
  end for
end Texture

```

Fig. 10. Algorithm 2.

evidence for this model comes from studies that suggest that a two-dimensional Gabor filter is a good model for the receptive fields of the neurons underlying texture perception. There are fundamental trade-offs in using texture for information display, between the precision with which the size and orientation at a point in a continuously varying texture region can be specified (or perceived) and the location of that packet of texture information. If location is specified precisely, then size and orientation can only be specified imprecisely, and vice versa. Given a constant texton density, if orientation is specified precisely, then size must be specified proportionately less precisely. In using texture we are not increasing the information density over that which is possible using color alone. Rather, we are trading spatial resolution for an increase in the number of display channels and display options.

There are many unresolved issues, in particular, those relating to the semantics of visual texture. Just as the luminance dimension of color space has certain perceptual characteristics that make it qualitatively different to the chromatic dimensions of color space, so is texture orientation qualitatively different from texture size. For example, texture orientation is useful for specifying vector field orientation [Van Wijk 1991], but texture contrast may be more useful to display such things as amount of energy.

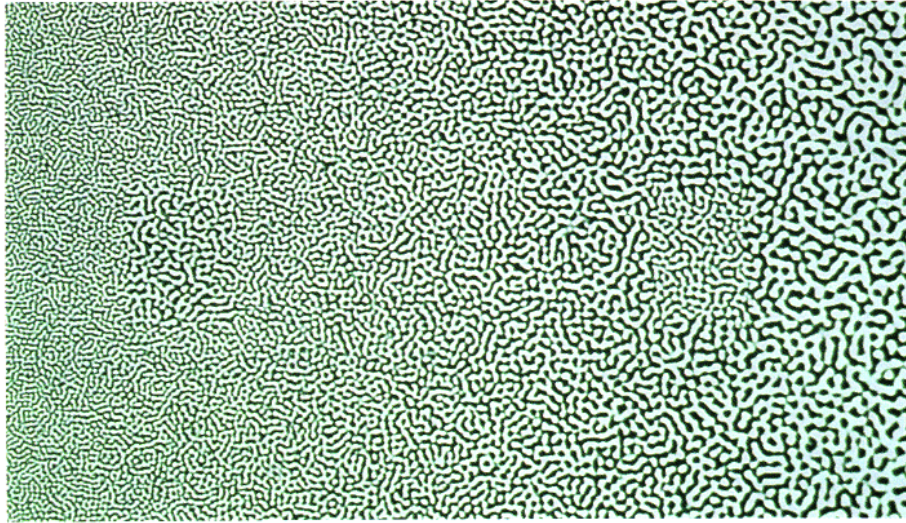


Fig. 11. Size illusion: Background texture varies from small on the left to large on the right. Two patches of identically sized texture are placed on the left and right of the center. The texture in the left patch appears larger grained than the texture in the right patch.

Some of the results that can be used to guide the use of visual texture are already known from studies in visual psychophysics (the review at the introduction of this paper barely scratches the surface of the available literature). However, these results are often inaccessible to those needing design guidelines because they are couched in the jargon of vision research. Much work is needed to bridge the gap between results in neurophysiology and psychophysics and the understanding of the designer of data displays.

It is quite clear from our experience that using texture effectively is at least as difficult as using color effectively, and that well-designed tools are needed to change the mapping of data variables to display variables. Nevertheless, the fact that texture has long been found to be essential in cartography [Bertin 1983] persuades us that a systematic method for manipulating texture variables in information displays is a significant advance.

APPENDIX. BASIC FOURIER ANALYSIS

This appendix is only a brief introduction. There is further material presented by Stein [1976] and Weaver [1983].

A space image, $F(\vec{x})$, can be built from frequency gratings as follows:

$$F(\vec{x}) = \frac{1}{\sqrt{2\pi}} \int \mathcal{F}(\vec{f}) \exp(-j\vec{f} \cdot \vec{x}) dw. \quad (17)$$

$\mathcal{F}(w)$ is called the Fourier transform of $F(x)$. (Using $-j$ rather than j is artificial but traditional.) Either F in the space domain or \mathcal{F} in the frequency domain specifies the image. For such an image as ripples on the water, the

Table II. Transformations in the Frequency Domain Induced by Transformations in the Space Domain

Formula	Space domain	Frequency domain
Objective function F and its transform \mathcal{F}	$F(\mathbf{x})$	$\mathcal{F}(\vec{\mathbf{f}})$
Translation in space: Center moved to \mathbf{x}_0	$F(\mathbf{x} - \mathbf{x}_0)$	$\exp(j\vec{\mathbf{f}} \cdot \mathbf{x}_0)\mathcal{F}(\vec{\mathbf{f}})$
Multiply the space function by a complex grating (translation in frequency)	$\exp(-j\vec{\mathbf{f}}_0 \cdot \mathbf{x})F(\mathbf{x})$	$\mathcal{F}(\vec{\mathbf{f}} - \vec{\mathbf{f}}_0)$
Scale (by scalar, s) (note the inverse scaling in the frequency domain)	$F(s\mathbf{x})$	$\mathcal{F}(\vec{\mathbf{f}}/s)$
Scale by diagonal matrix \mathbf{D}	$F(\mathbf{D}\mathbf{x})$	$\mathcal{F}(\mathbf{D}^{-1}\vec{\mathbf{f}})/\det(\mathbf{D})$
Rotation by R , a rotation matrix specifying orientation O	$F(\mathbf{R}\mathbf{x})$	$\mathcal{F}(R\vec{\mathbf{f}})$
Amplitude scaling by c (contrast)	$cF(\mathbf{x})$	$c\mathcal{F}(\vec{\mathbf{f}})$

frequency description can be more economical and easy to manipulate than the space description. $\mathcal{F}(\omega)$ is obtained from $F(x)$ by a similar integral,

$$\mathcal{F}(\vec{\mathbf{f}}) = \frac{1}{\sqrt{2\pi}} \int F(\mathbf{x}) \exp(j\vec{\mathbf{f}} \cdot \mathbf{x}) dx. \quad (18)$$

(The scaling factor, $(1/2\pi)$, can be distributed between transform and inverse transform in any way; the symmetric choice is not universal.)

(If $F(x)$ contains a pure sinusoid, $\mathcal{F}(\omega)$ will contain a delta function at the appropriate frequency, a mathematical complication beyond the scope of this paper. The delta function can always be approximated by a narrow peak.)

Transformations induced in the frequency domain by some simple transformations in the space domain are given in Table II.

REFERENCES

- BARLOW, H. B. 1972. Single units and sensation: A neuron doctrine for perceptual psychology? *Perception* 1, 3 (May), 371-394.
- BECK, J. 1983. Textural segmentation, second order statistics, and textural elements. *Biol. Cybern.* 48, 2 (April), 125-130.
- BERTIN, J. 1983. *Semiology of Graphics*, W. J. Berg, Transl. University of Wisconsin Press, Madison, Wis.
- BLAKE, R., AND HOOLIGAN, K. 1985. Orientation selectivity in cats and humans assessed by masking. *Vision Res.* 25, 10 (Oct.), 1459-1467.
- BLAKEMORE, C., AND CAMPBELL, F. W. 1969. On the existence of neurones in the human visual system selectively sensitive to the orientation and size of retinal images. *J. Physiol.* 203, 237-260.
- BLAKEMORE, C., NACHMIAS, J., AND SUTTON, P. 1970. The perceived spatial frequency shift: Evidence for frequency selective neurons in the human brain. *J. Physiol.* 210, 727-750.
- BOVIK, A. C., CLARK, M., AND GEISLER. 1990. Multichannel texture analysis using localized spatial filters. *IEEE Trans. Pattern Anal. Mach. Intell.* 12, 1 (Jan.), 55-73.
- CAELLI, T. M., AND BEVAN, P. 1983. Probing the spatial frequency spectrum for orientation sensitivity with stochastic textures. *Vision Res.* 23, 1 (Jan.), 39-45.
- CAELLI, T. M., BRETEL, H., RENTSCHLER, I., AND HILZ, R. 1983. Discrimination thresholds in the two-dimensional spatial frequency domain. *Vision Res.* 23, 2 (Feb.), 129-133.

- CAELLI, T. M., AND MORAGLIA, G. 1985. On the detection of Gabor signals and discriminations of Gabor textures. *Vision Res.* 25, 5 (May), 671–684.
- CAMPBELL, F. W., AND ROBSON, J. G. 1968. Application of Fourier analysis to the visibility of gratings. *J. Physiol.* 197, 551–566.
- CHUA, F. C. 1990. The processing of spatial frequency and orientation information. *Percept. Psychophysics* 47, 1 (Jan.), 79–86.
- DAUGMAN, J. G. 1985. Uncertainty relation for resolution in space, spatial frequency, and orientation optimized by two-dimensional visual cortical filters. *J. Opt. Soc. Am. 2A*, 7, 1160–1169.
- DAUGMAN, J. G. 1984. Spatial visual channels in the Fourier plane. *Vision Res.* 24, 9 (Sept.), 91–910.
- GARNER, W. R., AND FELFOLDY, G. L. 1970. Integrality of stimulus dimensions in various types of information processing. *Cognitive Psychol.* 1, 3 (Aug.), 225–241.
- HARVEY, L. O., AND GERVAIS. 1981. Internal representation of visual texture as the basis for the judgement of similarity. *J. Exp. Psychol: Human Perception Perform.* 7, 4 (July), 741–753.
- HEELEY, D. 1991. Spatial frequency difference thresholds depend on stimulus area. *Spat. Vision* 5, 3 (July), 205–217.
- HUEBEL, D. H., AND WIESEL, T. 1968. Receptive fields and functional architecture of monkey striate cortex. *J. Physiol.* 195, 215–243.
- JONES, J., AND PALMER, L. 1987. An evaluation of the two-dimensional Gabor filter model of simple receptive fields in the cat striate cortex. *J. Neurophysiol.* 59, 1233–1258.
- JULESZ, B. 1975. Textons, the elements of texture perception and their interactions. *Nature* 290, 5802 (March), 91–97.
- MARCELJA, S. 1980. Mathematical descriptions of the responses of simple cortical cells. *J. Opt. Soc. Am.* 70, 11 (Nov.), 1297–1300.
- MITCHELL, D. E., FREEMAN, R., AND WESTHEIMER, G. 1967. Effect of orientation on the modulation sensitivity for interference fringes on the retina. *J. Opt. Soc. Am.* 57, 245–249.
- NOTHDURFT, H. C. 1991. Different effects from spatial frequency masking in texture segregation and texton detection tasks. *Vision Res.* 31, 2 (Feb.), 299–320.
- PORAT, M., AND ZEEVI, Y. Y. 1989. Localized texture processing in vision: Analysis and synthesis in Gaborian space. *IEEE Trans. Biomed. Eng.* 36, 1 (Jan.), 115–129.
- SAGI, D. 1990. Detection of an orientation singularity in Gabor textures: Effect of signal density and spatial frequency. *Vision Res.* 30, 9 (Sept.), 1377–1388.
- SMITH, A. R. 1979. Color gamut transform pairs. *Comput. Graph.* 13, 2 (July), 12–19.
- STEIN, E. M. 1976. Harmonic analysis on R^n . In *Studies in Harmonic Analysis*, J. H. Ash, Ed. Studies in Mathematics, vol. 13. Mathematical Association of America, Washington, D.C., 237–243.
- VAN WIJK, J. J. 1991. Spot noise: Texture synthesis for data visualization. *Comput. Graph.* 25, 4 (July), 309–318.
- WAINER, H., AND FRANCOLINI, C. M. 1980. An empirical enquiry concerning human understanding of two variable color maps. *Am. Stat.* 34, 2 (Feb.), 81–93.
- WARE, C. 1988. Color sequences for univariate maps: Theory, experiments and principles. *IEEE Comput. Graph. Appl.* 8, 5 (May), 41–49.
- WARE, C., AND COWAN, W. 1990. The RGYB color geometry. *ACM Trans. Graph.* 9, 2, 226–232.
- WARE, C., AND KNIGHT, W. 1992. Orderable dimensions of visual texture for data display: Orientation, size and contrast. In *ACM SIGCHI'92 Proceedings* (Monterey, Calif.). ACM, New York, 203–210.
- WEAVER, H. J. 1983. *Application of Discrete and Continuous Fourier Analysis*. Wiley, New York.
- WILSON, H. R., AND BERGEN, J. R. 1979. A four mechanism model for threshold spatial vision. *Vision Res.* 19, 1 (Jan.), 19–32.
- WYSZECKI, G., AND STILES, W. S. 1982. *Color Science: Concepts and Methods, Quantitative Data and Formulae*. Wiley, New York.

Received February 1992; revised October 1993 and November 1994; accepted July 1994